Molecular Diversity (2022) 26:2863–2876
https://doi.org/10.1007/s11030-022-10476-8

ORIGINAL ARTICLE

Synthesis of novel carboxamide- and carbohydrazide-benzimidazoles as selective butyrylcholinesterase inhibitors

Ozum Ozturk[2] · Fathima Manaal Farouk[1] · Luyi Ooi[1] · Christine Shing Wei Law[1] · Muhammed Tilahun Muhammed[3] · Esin Aki-Yalcin[2] · Keng Yoon Yeong[1]

Received: 26 August 2021 / Accepted: 31 May 2022 / Published online: 2 July 2022

Abstract

Selectively inhibiting butyrylcholinesterase (BChE) is hypothesized to help in the management of Alzheimer's disease (AD). Several studies have determined a correlation between the increased activity of BChE and the onset of AD. An advantage of BChE over acetylcholinesterase inhibition is that absence of BChE activity does not lead to obvious physiological disturbance. However, currently no BChE inhibitors are available commercially as potential therapeutics for AD. In our continuous effort to find potent BChE inhibitors for Alzheimer's disease, a total of 22 novel benzimidazoles with diversified substitutions were synthesized and evaluated for their anticholinesterase activities in this study. Among the synthesized compounds, **2j** and **3f** were found to exhibit potent and selective BChE inhibition with IC_{50} values of 1.13 and 1.46 µM, respectively. Molecular docking studies were carried out to rationalize the observed inhibitory activities. The compounds were predicted to have high penetration across the blood–brain barrier. Moreover, cell proliferative studies were also performed to evaluate the toxicity profile of the interested compounds.

Graphical abstract

Compound **3f** was found to be a potent and selective butyrylcholinesterase inhibitor with an IC_{50} value of 1.46 µM.

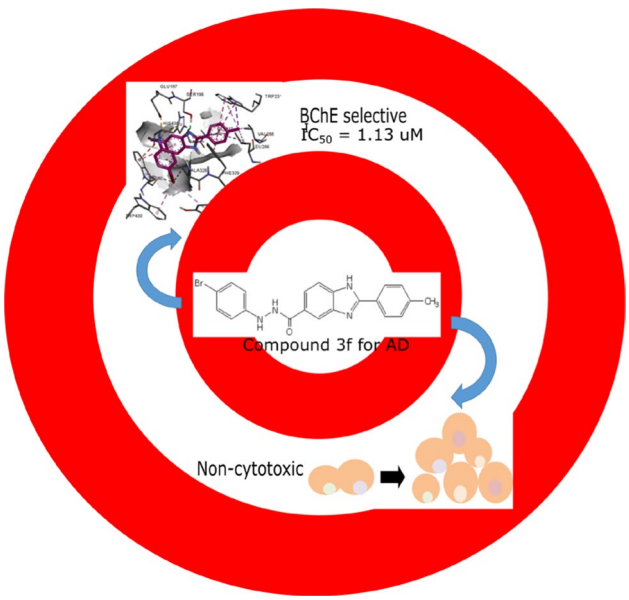

Keywords Alzheimer's disease · Benzimidazole · Cholinesterase inhibitors · Cytotoxicity · Molecular docking

Extended author information available on the last page of the article

Introduction

Alzheimer's disease (AD) is a progressive neurodegenerative disease and the main cause of dementia. As the disease progresses, cognitive and memory decline are observed. It will ultimately lead to death if left untreated. The lack of clear evidence in what causes AD hampers the effort to find treatment for this disease. Nevertheless, several theories were proposed to explain the pathophysiological and molecular changes during the disease progression. Cholinergic disruption is hypothesized to be one of the causes of AD [1, 2]. It is thus presumed that blocking the cholinergic degeneration in the brain would delay or prevent the onset of AD. In fact, this has been an important therapeutic approach in AD research for the past 30 years [3]. More recently, positive correlations have been reported between cholinergic dysfunction and the deposition of amyloid beta (Aβ) plaques and neurofibrillary tangles (NFT) [4, 5], which are the two major hallmarks of AD. These findings gave a new perspective to cholinesterase inhibitors in AD therapy.

Therapeutics drugs developed to enhance the cholinergic activity involved the inhibition of the acetylcholine-hydrolysing enzymes, such as acetylcholinesterase (AChE) and butyrylcholinesterase (BChE). Current cholinesterase inhibitors (donepezil, galantamine and rivastigmine) [4], however, are capable of only minimizing the symptoms when administered during the prodromal stages and have positive effects only for a short period of time (1–3 years) [6]. Due to the short-term effects of the drugs and their side effects, there is a need to look into developing new cholinesterase inhibitors from a different perspective. Various chemical structures such as triazoles [7] and benzimidazoles [8–10] have been researched for use as cholinesterase inhibitors. Benzimidazoles, in particular, have been receiving significant attention due to some promising reported results, especially as selective BChE inhibitors [1, 8]. Inhibiting BChE has recently been postulated to play an important role in the management of AD [11, 12].

In this study, we aim to develop potent and selective butyrylcholinesterase inhibitors based on the benzimidazole scaffold. Cholinesterase activity was measured using a modified Ellman's method while cell proliferative assay was also carried out to evaluate the cytotoxicity of the synthesized compounds. Moreover, molecular docking studies and preliminary in silico ADME predictions of the active compounds were conducted.

Materials and methods

Chemistry

General procedure for the preparation of 2-(4-substituedphenyl)-N-(3/4-substituedphenyl)-1H-benzimidazol-5-carboxamide derivatives.

2-(4-substitutedphenyl)-benzimidazole-5-carboxylic acid derivative (1 mmol) was heated in a magnetic stirrer at 80 °C for 6 h under reflux in thionyl chloride. After the reaction, excess thionyl chloride was evaporated. Obtained 2-(4-substitutedphenyl)-benzimidazole-5-carbonyl chloride derivatives were dissolved in anhydrous diethyl ether (10 mL) and then were added dropwise to the mixture of 3/4-substitued aniline (1 mmol), sodium bicarbonate (2 mmol), ether (10 mL) and water (10 mL). The mixture was stirred overnight in an ice bath, then filtered and washed with water, 2 N HCl and ether, respectively. The residues were recrystallized from EtOH and the obtained 2-(4-substituedphenyl)-N-(3/4-substituedphenyl)-1H-benzimidazol-5-carboxamide derivatives were dried in vacuo [13].

General procedure for the preparation of N'-(4-substituedphenyl)-2-(4-substitutedphenyl)-1H-benzimidazol-5-carbohydrazide derivatives.

The procedure to obtain 2-(4-substitutedphenyl)-benzimidazole-5-carbonyl chloride derivatives was the same as the above. These derivatives were dissolved in anhydrous diethyl ether (10 mL) and then were added dropwise to the mixture of 4-substituedhydrazine (1 mmol), sodium bicarbonate (2 mmol), ether (10 mL) and water (10 mL). The mixture was stirred overnight in an ice bath, then filtered and washed with water, 2 N HCl and ether, respectively. The residues recrystallized from ethanol and obtained N'-(4-substituedphenyl)-2-(4-substituedphenyl)-1H-benzimidazol-5-carbohydrazide derivatives were dried in vacuo.

N-(4-chlorophenyl)-2-(4-hydroxyphenyl)-1H-benzimidazole-5-carboxamide (2a)

34% yield; mp 274–277 °C; ^{1}H NMR (DMSO-d_6, 400 MHz): $\delta = 7.07$ (d, 2H, $J_o = 8.8$ Hz, H-3', 5'), 7.41 (d, 2H, $J_o = 8.8$ Hz, H-3″, 5″), 7.84 (d, 3H, H-7, 2″, 6″), 8.06 (d, 1H, $J_o = 8.8$ Hz, H-6), 8.21 (d, 2H, $J_o = 8.8$ Hz, H-2', 6'), 8.31 (s, 1H, H-4), 10.63 (s, 1H, N–H); ^{13}C NMR (DMSO-d_6, 100 MHz): $\delta = 113.28$, 113.45, 116.45, 121.98, 125.01, 127.34, 128.46, 130.47, 131.55, 131.86,

134.17, 138.03, 151.03, 162.52, 164.79; MS (ESI) *m/z* 364.5 [$M^+ + H$] (100), 366.5 [$M^+ + H + 2$] (50).

N-(4-methoxyphenyl)-2-(4-hydroxyphenyl)-1H-benzimidazole-5-carboxamide (2b)

35% yield; mp 300–302 °C; ^{1}H NMR (DMSO-d_6, 400 MHz): $\delta = 3.74$ (s, 3H, –CH_3), 6.94 (d, 2H, $J_o = 8.8$ Hz, H-3', 5'), 7.09 (d, 2H, $J_o = 8.8$ Hz, H-3″, 5″), 7.70 (d, 2H, $J_o = 8.8$ Hz, H-2″, 6″), 7.85 (d, 1H, $J_o = 8.4$ Hz, H-7), 8.09 (dd, 1H, $J_o = 8.4$ Hz, $J_m = 1.6$, H-6), 8.29 (d, 2H, $J_o = 8.8$ Hz, H-2', 6'), 8.32 (s, 1H, H-4), 10.43 (s, 1H, N–H); ^{13}C NMR (DMSO-d_6, 100 MHz): $\delta = 55.19$, 113.25, 113.30, 113.41, 113.74, 116.52, 122.18, 124.99, 130.53, 131.81, 132.09, 132.11, 133.92, 150.91, 155.65, 162.59, 164.30; MS (ESI) *m/z* 360.5 [$M^+ + H$] (100).

N-(4-trifluoromethylphenyl)-2-(4-hydroxyphenyl)-1H-benzimidazole-5-carboxamide (2c)

34% yield; mp 300–302 °C; ^{1}H NMR (DMSO-d_6, 400 MHz): $\delta = 7.05$ (d, 2H, $J_o = 8.8$, H-3', 5'), 7.46 (d, 1H, $J_o = 8$ Hz, H-4″), 7.61 (t, 1H, H-5″), 7.82 (d, 1H, $J_o = 8.4$ Hz, H-7), 8.04 (dd, 1H, $J_o = 8.8$ Hz, $J_m = 1.2$ Hz, H-6), 8.08 (d, 1H, $J_o = 8.4$ Hz, H-6″), 8.15 (d, 2H, $J_o = 8.4$ Hz, H-2', 6'), 8.30 (s, 1H, H-2″), 8.32 (s, 1H, H-4), 10.75 (s, 1H, N–H); COSY [δH/δH]: 7.46/7.61 [H-4″/H-5″], 7.05/8.15 [H-2',6'/H-3',5'], 7.61/8.08 [H-5″/H-6″], 7.82/8.04 [H-7/H-6]; MS (ESI) *m/z* 398.5 [$M^+ + H$] (100).

N,2-bis(4-methoxymethyl)-1H-benzimidazole-5-carboxamide (2d)

31% yield; mp 276–280 °C; ^{1}H NMR (DMSO-d_6, 400 MHz): $\delta = 3.73$ (s, 3H, –CH_3), 3.88 (s, 3H, –CH_3), 6.92 (d, 2H, $J_o = 7.2$ Hz, H-3″, 5″), 7.25 (d, 2H, $J_o = 8.8$ Hz, H-3', 5'), 7.69 (d, 2H, $J_o = 7.2$ Hz, H-2″, 6″), 7.84 (d, 1H, $J_o = 8.4$ Hz, H-7), 8.08 (dd, H, $J_o = 8.4$ Hz, $J_m = 1.2$ Hz, H-6), 8.32 (d, 1H, $J_m = 1.2$ Hz, H-4), 8,39 (d, 2H, $J_o = 9.2$ Hz, H-2', 6'), 10.42 (s, 1H, N–H); ^{13}C NMR (DMSO-d_6, 100 MHz): $\delta = 55.18$, 55.82, 113.36, 113.46, 113.73, 115.15, 115.32, 122.17, 125.00, 130.33, 131.99, 132.10, 132.12, 134.09, 150.54, 155.64, 163.32, 164.27; MS (ESI) *m/z* 374.3 [$M^+ + H$] (100).

N-(4-chlorophenyl)-2-(4-methoxyphenyl)-1H-benzimidazole-5-carboxamide (2e)

29% yield; mp 301–305 °C; ^{1}H NMR (DMSO-d_6, 400 MHz): $\delta = 3.90$ (s, 3H, –CH_3), 7.26 (d, 2H, $J_o = 8.4$ Hz, H-3', 5'), 7.43 (d, 2H, $J_o = 8$ Hz, H-3″, 5″), 7.84–7.89 (m, 3H, H-7, 2″, 6″), 8.08 (dd, 1H, $J_o = 8.8$ Hz, $J_m = 1.6$ Hz, H-6), 8.35 (s, 1H, H-4), 8.39 (d, 2H, H-2', 6'), 10.67 (s, 1H, N–H); ^{13}C NMR (DMSO-d_6, 100 MHz): $\delta = 55.65$, 113.40, 113.76, 114.94, 116.19, 121.95, 124.55, 127.25, 128.34, 129.98, 131.13, 132.97, 135.22, 138.04, 150.99, 162.94, 164.86; MS (ESI) *m/z* 378.3 [$M^+ + H$] (100), 379.4 [$M^+ + H + 1$] (40).

N-(4-hydroxyphenyl)-2-(4-methoxyphenyl)-1H-benzimidazole-5-carboxamide (2f)

49% yield; mp 288–292 °C; ^{1}H NMR (DMSO-d_6, 400 MHz): $\delta = 3.84$ (s, 3H, -CH_3), 6.75 (d, 2H, $J_o = 9.2$ Hz, H-3″, 5″), 7.26 (d, 2H, $J_o = 8.4$ Hz H-3', 5'), 7.54 (d, 2H, $J_o = 8.4$ Hz, H-2″, 6″), 7.84 (d, 1H, $J_o = 8$ Hz, H-7), 8.07 (d, 1H, $J_o = 8.8$ Hz, H-6), 8.31 (s, 1H, H-4), 8.37 (d, 2H, $J_o = 8.4$ Hz, H-2' ve 6'), 10.31(s, 1H, N–H); ^{13}C NMR (DMSO-d_6, 100 MHz): $\delta = 113.36$, 114.98, 115.16, 115.45, 122.43, 124.93, 130.27, 130.54, 132.22, 134.14, 150.59, 153.86, 163.28, 164.14; MS (ESI) *m/z* 360.3 [$M^+ + H$] (100).

N-(4-bromophenyl)-2-(4-methoxyphenyl)-1H-benzimidazole-5-carboxamide (2 g)

36% yield; mp 310–313 °C; ^{1}H NMR (DMSO-d_6, 400 MHz): $\delta = 3.83$ (s, 3H, –CH_3), 7.29 (d, 2H, $J_o = 9.2$ Hz, H-3', 5'), 7.56 (d, 2H, $J_o = 8$ Hz, H-3″,5″), 7.82 (d, 2H, $J_o = 6.8$ Hz, H-2″, 6″), 7.87 (d, 1H, $J_o = 8.8$ Hz, H-7), 8.08 (dd, 1H, $J_o = 8.8$, Hz, $J_m = 1.6$ Hz, H-6), 8.34–8.37 (m, 3H, H-4, 2', 6'), 10.65 (s, 1H, N–H); ^{13}C NMR (DMSO-d_6, 100 MHz): $\delta = 55.71$, 113.25, 113.61, 115.04, 115.37, 122.31, 124. 94, 130.21, 131.30, 131.47, 132.12, 134.43, 138.42, 163.19, 164.74, 150.68; MS (ESI) *m/z* 422.5 [$M^+ + H$] (95), 424.6 [$M^+ + H + 2$] (100).

N-(3-methoxyphenyl)-2-(4-methoxyphenyl)-1H-benzimidazole-5-carboxamide (2 h)

39% yield; mp 201–205 °C; ^{1}H NMR (DMSO-d_6, 400 MHz): $\delta = 3.15$ (s, 3H, –CH_3), 3.46 (s, 3H, –CH_3), 6.65 (dd, 1H, $J_o = 8.4$ Hz, $J_m = 2.4$ Hz, H-4″), 7.13 (d, 2H, $J_o = 9.2$ Hz H-3', 5'), 7.23 (t,1H, H-5″), 7.39 (dd, 1H, $J_o = 8.4$ Hz, $J_m = 0.8$ Hz, H-6″), 7.51 (m, 1H, H-2″), 7.65 (d, 1H, $J_o = 8.4$ Hz, H-7), 7.83 (dd, 1H, $J_o = 8.0$ Hz, $J_m = 1.6$ Hz, H-6), 8.15 (d, 2H, $J_o = 8.4$ Hz, H- 2', 6'), 8.21 (s, 1H, H-4), 10.21 (s, 1H, N–H); COSY [δH/δH]: 6.65/7.23 [H- 4″/H-5″], 7.13/8.15 [H-2',6'/H-3',5'], 7.23/7.39 [H-5″/H-6″], 7.65/7.83 [H-7/H-6]; ^{13}C NMR (DMSO-d_6, 100 MHz): $\delta = 54.99$, 55.41, 106.00, 108.92, 112.54, 114.53, 121.58, 122.20, 128.49, 128.86, 129.32, 140.68, 153.19, 159.43, 161.18, 165.89; MS (ESI) *m/z* 374.5 [$M^+ + H$] (100).

N-(4-chlorophenyl)-2-(4-methylphenyl)-1H-benzimidazole-5-carboxamide (2i)

45% yield; mp 325–326 °C; ^{1}H NMR (DMSO-d_6, 400 MHz): $\delta = 2.41$ (s, 3H, –CH_3), 7.39 (d, 2H, $J_o = 7.2$ Hz, H-3', 5'),

7.48 (d, 2H, J_o = 8 Hz, H-3″, 5″), 7.83–7.86 (m, 3H, H-7, 2″, 6″), 8.05 (dd, 1H, J_o = 8.4 Hz, J_m = 1.6 Hz, H-6), 8.26 (d, 2H, J_o = 8 Hz, H-2',6'), 8.34 (d, 1H, J_m = 1.2 Hz, H-4), 10.62 (s, 1H, N–H); ^{13}C NMR (DMSO-d_6, 100 MHz): δ = 21.13, 113.71, 114.11, 121.74, 121.96, 124.59, 127.27, 127.88, 128.41, 129.96, 131.13, 133.44, 135.66, 138.10, 143.30, 151.27, 164.95; MS (ESI) *m/z* 362.4 [M^+ + H] (100), 364.4 [M^+ + H + 2] (33).

N-(4-hydroxyphenyl)-2-(4-methylphenyl)-1H-benzimidazole-5-carboxamide (2j)

49% yield; mp 341–342 °C; ^{1}H NMR (DMSO-d_6, 400 MHz): δ = 2.43 (s, 3H, –CH_3), 6.75 (d, 2H, J_o = 7.2 Hz, 3″, 5″), 7.50 (d, 2H, J_o = 8 Hz, H-3', 5'), 7.55 (d, 2H, J_o = 8.8 Hz, H-2″, 6″), 7.86 (d, 1H, J_o = 8.8 Hz, H-7), 8.08 (dd, 1H, J_o = 8.4 Hz, J_m = 1.6 Hz, H-6), 8.29 (d, 2H, J_o = 8.4 Hz, H-2', 6'), 8.33 (d, 1H, H-4), 10.32 (s, 1H, N–H); COSY [δH/δH]: 6.75/7.55 [H-3″,5″/H-2″,6″], 7.50/8.29 [H-3',5'/H-2',6'], 7.86/8.08 [H-7/H-6]; NOESY: 7.55/10.32 [H-2″,6″/H-NH]; ^{13}C NMR (DMSO-d_6, 100 MHz): δ = 21.25, 113.59, 113.63, 115.00, 120.65, 122.46, 125.12, 128.19, 130.16, 130.55, 132.16, 132.40, 134.17, 144.07, 150.66, 153.66, 153.90, 164.12; MS (ESI) *m/z* 344.5 [M^+ + H] (100).

N-(4-methoxyphenyl)-2-(4-methylphenyl)-1H-benzimidazole-5-carboxamide (2 k)

20% yield; mp 285–286 °C; ^{1}H NMR (DMSO-d_6, 400 MHz): δ = 2.40 (s, 3H, 4' –CH_3), 3.72 (s, 3H, 4″–CH_3), 6.91 (d, 2H, J_o = 9.2 Hz, H-3″, 5″), 7.49 (d, 2H, J_o = 8 Hz, H-3′, 5′), 7.69 (d, 2H, J_o = 9.2 Hz, H-2″, 6″), 7.86 (d, 1H, J_o = 8.8 Hz, H-7), 8.08 (d, 1H, J_o = 8.4 Hz, H-6), 8.29 (d, 2H, J_o = 8 Hz, H-2', 6'), 8.34 (s, 1H, H-4), 10.42 (s, 1H, N–H); ^{13}C NMR (DMSO-d_6, 100 MHz): δ = 21.16, 55.10, 113.53, 113.64, 120.68, 122.09, 124.99, 128.09, 130.04, 132.05, 132.09, 132.21, 134.27; MS (ESI) *m/z* 358.3 [M^+ + H] (100).

N-(3-methoxyphenyl)-2-(4-methylphenyl)-1H-benzimidazole-5-carboxamide (2 l)

23% yield; mp 285–286 °C; ^{1}H NMR (DMSO-d_6, 400 MHz): δ = 2.40 (s, 3H, 4'–CH_3), 3.74 (s, 3H, 4″–CH_3), 6.68 (dd, 1H, J_o = 8 Hz, J_m = 2 Hz, H-4″), 7.24 (t, 1H, H-5″), 7.40 (d, 1H, J_o = 8 Hz, J_m = 1.6 Hz, H-6″), 7.50 (d, 2H, J_o = 6.8 Hz, H-3', 5'), 7.87 (d, 1H, J_o = 8.4 Hz, H-7), 8.09 (dd, 1H, J_o = 8.4 Hz, J_m = 1.6 Hz, H-6), 8.31(d, 2H, J_o = 8.4 Hz, H-2', 6'), 8.36 (s, 1H, H-4), 10.52 (s, 1H, N–H); COSY [δH/δH]: 2.41/7.50 [CH_3(4')/H-3',5'], 6.68/7.24 [H-4″/H-5″], 7.24/7.40 [H-5″/H-6″], 7.50/8.31 [H-3',5'/H-2',6'], 7.87/8.09 [H-7/H-6]; ^{13}C NMR (DMSO-d_6, 100 MHz): δ = 21.23, 55.02, 106.24, 109.27, 112.73, 113.63, 113.88, 120.74, 125.15, 128.18, 129.36, 130.12, 132.04, 132.29, 134.46, 140.29, 144.01, 150.80, 159.40, 164.76; MS (ESI) *m/z* 358.61 [M^+ + H] (100).

N-(4-methoxyphenyl)-2-(4-bromophenyl)-1H-benzimidazole-5-carboxamide (2 m)

30% yield; mp 288–292 °C; ^{1}H NMR (DMSO-d_6, 400 MHz): δ = 3.73 (s, 3H, –CH_3), 6.91 (d, 2H, J_o = 9.2 Hz, H-3″, 5″), 7.69 (d, 2H, J_o = 9.2 Hz, H-3', 5'), 7.85 (d, 1H, J_o = 8.8 Hz, H-7), 7.91 (d, 2H, J_o = 8.4 Hz, H-2″, 6″), 8.07 (dd, 1H, J_o = 8.8 Hz, J_m = 1.2 Hz, H-6), 8.32 (d, 2H, J_o = 8.8 Hz, H-2', 6'), 8.36 (s, 1H, H-4), 10.39 (s, 1H, N–H); ^{13}C NMR (DMSO-d_6, 100 MHz): δ = 55.16, 113.69, 113.88, 114.18, 122.12, 124.38, 124.52, 126.31, 129.68, 131.64, 132.16, 132.42, 134.04, 136.00, 150.31, 155.59, 164.46; MS (ESI) *m/z* 422.4 [M^+ + H] (100), 424.4 [M^+ + H + 2] (95).

N-(3-nitrophenyl)-2-(4-bromophenyl)-1H-benzimidazole-5-carboxamide (2n)

32% yield; mp 303–307 °C; ^{1}H NMR (DMSO-d_6, 400 MHz): δ = 7.64 (t, 1H, H-5″), 7.76 (d, 1H, J_o = 8 Hz, H-7), 7.82 (d, 2H, J_o = 8.8 Hz, H-3', 5'), 7.92–7.97 (m, 2H, H-4″, 6), 8.17 (d, 2H, J_o = 8.4 Hz, H-2', 6'), 8.22 (dd, 1H, J_o = 8.4 Hz, J_m = 1.6 Hz, H-6″), 8.33 (s, 1H, H- 4), 8.84 (m, 1H, H-2″), 10.78 (s, 1H, N–H); COSY [δH/δH]: 7.64/7.92 [H-5″/H-4″], 7.64/8.22 [H-5″/H-6″], 7.82/8.17 [H-3',5'/H-2',6'], 7.76/7.97 [H-7/H-6]; ^{13}C NMR (DMSO-d_6, 100 MHz): δ = 114.28, 115.36, 117.89, 123.18, 124.67, 126.13, 127.32, 128.92, 129.92, 132.16, 139.68, 140.52, 147.83, 151.85, 154.58, 165.95; MS (ESI) *m/z* 437.4 [M^+ + H] (100), 439.7 [M^+ + H + 2] (50).

N-(4-chlorophenyl)-2-(4-bromophenyl)-1H-benzimidazole-5-carboxamide (2o)

28% yield; mp 269–270 °C; MS (ESI) *m/z* 426.4 [M^+ + H] (80), 428.3 [M^+ + H + 2] (100).

N-(4-nitrophenyl)-2-(4-hydroxyphenyl)-1H-benzimidazole-5-carbohydrazide (3a)

31% yield; mp 236–239 °C; ^{1}H NMR (DMSO-d_6, 400 MHz): δ = 6.85 (d, 2H, J_o = 8.8 Hz, H-3', 5'), 7.07 (d, 2H, J_o = 8.8 Hz, H-2″, 6″), 7.85 (d, 1H, J_o = 8.4 Hz, H-7), 8.03 (dd, 1H, J_o = 8.8 Hz, J_m = 1.2 Hz, H-6), 8.08 (d, 2H, J_o = 8.8 Hz, H-3″, 5″) 8.21 (d, 2H, J_o = 8.8 Hz, H-2', 6'), 8.28 (s, 1H, H-4), 9.29 (s, 1H, N'-H), 10.9 (s, 1H, N–H); ^{13}C NMR (DMSO-d_6, 100 MHz): δ = 110.77, 113.24, 113.57, 113.64, 116.52, 124.68, 125.96, 129.15, 130.53,132.13, 134.61, 138.14,151.21, 154.97, 162.57, 165.59; MS (ESI) *m/z* 390.5 [M^+ + H] (100).

N-(4-nitrophenyl)-2-(4-methoxyphenyl)-1H-benzimidazole-5-carbohydrazide (3b)

27% yield; mp 273–276 °C; ^{1}H NMR (DMSO-d_6, 400 MHz): δ = 3.87 (s, 3H, –CH_3), 6.85 (d, 2H, J_o = 8.8 Hz, H-3′ ve 5′), 7.23 (d, 2H, J_o = 9.2 Hz, H-2″, 6″), 7.80 (d, 1H, J_o = 8.4 Hz, H-7), 7.97 (d, 1H, J_o = 8.4 Hz, H-6), 8.08 (d, 2H, J_o = 9.6 Hz, H-2', 6'), 8.26–8.28 (m, 3H, 4, H-3″, 5″), 9.28 (s, H, N'-H), 10.83 (s, 1H, N–H); ^{13}C NMR (DMSO-d_6, 100 MHz): δ = 55.72, 110.76, 113.76, 113.97, 114.99, 117.39, 123.84, 125.97, 128.26, 129.76, 134.35, 136.78, 138.12, 151.68, 155.07, 162.67, 165,94; MS (ESI) *m/z* 404.4 [M^+ + H] (100).

N-(4-bromophenyl)-2-(4-methoxyphenyl)-1H-benzimidazole-5-carbohydrazide (3c)

19% yield; mp 288–292 °C; ^{1}H NMR (DMSO-d_6, 400 MHz): δ = 3.87 (s, 3H, –CH_3), 6.85 (d, 2H, J_o = 8 Hz, H-3', 5'), 7.24–7.30 (m, 4H, H-2″, 3″, 5″ ve 6″), 7.85 (d, 1H, J_o = 8.8 Hz, H-7), 8.04 (dd, 1H, J_m = 1.2 Hz, J_o = 8.4 Hz, H-6), 8.30 (s, 1H, H-4), 8.41 (d, 2H, J_o = 9.2 Hz, H-2', 6'), 10.66 (s, 1H, N–H); ^{13}C NMR (DMSO-d_6, 100 MHz): δ = 55.75, 109.39, 113.18, 113.59, 114.28, 115.07, 115.46, 124.50, 129.70, 130.26, 131.29, 132.25, 134.54, 148.73, 150.65, 163.23, 165.59; MS (ESI) *m/z* 437.48 [M^+ + H] (100), 439.55, [M^+ + H + 2] (100).

N-(4-chlorophenyl)-2-(4-methoxyphenyl)-1H-benzimidazole-5-carbohydrazide (3d)

28% yield; mp 269–271 °C; ^{1}H NMR (DMSO-d_6, 400 MHz): δ = 3.88 (s, 3H, –CH_3), 6.81 (d, 2H, J_o = 8.8 Hz, H-3', 5'), 7.17 (d, 2H, J_o = 8.4 Hz, H-2″, 6″), 7.25 (d, 2H, J_o = 8.8 Hz, H-3″, 5″), 7.85 (d, 1H, J_o = 8.8 Hz, H-7), 8.05 (d, 1H, J_o = 8.4 Hz, H-6), 8.31 (s, 1H, H-4), 8.42 (d, 2H, J_o = 8.4 Hz, H-2', 6'), 10.67 (s, 1H, N–H); ^{13}C NMR (DMSO-d_6, 100 MHz): δ = 55.75, 113.17, 113.57, 113.78, 115.07, 115.32, 121.91, 124.56, 128.45, 129.79, 130.30, 132.11, 134.39, 148.32, 150.57, 163.27, 165.60; MS (ESI) *m/z* 393.5 [M^+ + H] (100), 395.5 [M^+ + H + 2] (33).

N-(4-chlorophenyl)-2-(4-methylphenyl)-1H-benzimidazole-5-carbohydrazide (3e)

37% yield; mp 284–285 °C; ^{1}H NMR (DMSO-d_6, 400 MHz): δ = 2.44 (s, 3H, –CH_3), 6.82 (d, 2H, J_o = 6.8 Hz, H-3', 5'), 7.20 (d, 2H, J_o = 6.8 Hz, H-2″, 6″), 7.53 (d, 2H, J_o = 8.4 Hz, H-3″, 5″), 7.90 (d, 1H, J_o = 8.8 Hz, H-7), 8.08 (dd, 1H, J_o = 8.4 Hz, J_m = 1.2 Hz, H-6), 8.33–8.35 (m, 3H, H-4, 2' ve 6'), 10.73 (s, 1H, N–H); ^{13}C NMR (DMSO-d_6, 100 MHz): δ = 21.24, 113.48, 113.82, 113.90, 120.73, 121.95, 124.73, 128.20, 128.54, 129.91, 130.13, 132.37, 134.63; MS (ESI) *m/z* 377.5 [M^+ + H] (100), 379.5 [M^+ + H + 2] (40).

N-(4-bromophenyl)-2-(4-methylphenyl)-1H-benzimidazole-5-carbohydrazide (3f)

21% yield; mp 282–283 °C; ^{1}H NMR (DMSO-d_6, 400 MHz): δ = 2.44 (s, 3H, –CH_3), 6.78 (d, 2H, J_o = 8.4 Hz, H-3', 5'), 7.31 (d, 2H, J_o = 8.8 Hz, H-2″, 6″), 7.53 (d, 2H, J_o = 8 Hz, H-3″, 5″), 7.89 (d, 1H, J_o = 8.4 Hz, H-7), 8.07 (d, 1H, J_o = 8.4 Hz, H-6), 8.32 (d, 2H, J_o = 8 Hz, H-2', 6'), 8.34 (s, 1H, H-4) 10.73 (s, 1H, N–H); ^{13}C NMR (DMSO-d_6, 100 MHz): δ = 21.24, 109.46, 113.53, 113.95, 114.34, 121.01, 124.61, 128.13, 129.76, 130.13, 131.39, 132.67, 134.94, 143.89, 148.82, 150.95, 169.69; MS (ESI) *m/z* 421.4 [M^+ + H] (100), 423.3 [M^+ + H + 2] (85).

N,2-bis(4-bromophenyl)-1H-benzimidazole-5-carbohydrazide (3 g)

26% yield; mp 303–307 °C; ^{1}H NMR (DMSO-d_6, 400 MHz): δ = 6.78 (d, 2H, J_o = 8.4 Hz, H-2″, 6″), 7.32 (d, 2H, J_o = 8.4 Hz, H-3″,5″), 7.89 (d, 1H, J_o = 8.4 Hz, H-7), 7.95 (d, 2H, J_o = 8.8 Hz, H-3', 5'), 8.05 (d, 1H, J_o = 8.4 Hz, H-6), 8.33–8.35 (m, 3H, H-4, 2', 6'), 10.68 (s, 1H, N–H); ^{13}C NMR (DMSO-d_6, 100 MHz): δ = 109.27, 109.52, 114.29, 121.98, 123.78, 126.93, 128.58, 128.89, 131.33, 132.07, 133.96, 149.10, 152.18, 166.66; MS (ESI) *m/z* 485.4 [M^+ + H] (50), 487.5 [M^+ + H + 2] (100), 489.5 [M^+ + H + 5] (55).

In vitro *cholinesterase inhibition assay*

All reagents used in this assay were of analytical grade. Acetylcholinesterase (AChE) from electric eel, butyrylcholinesterase (BChE) from equine serum, S-butyrylthiocholine iodide and acetylthiocholine iodide were purchased from Sigma-Aldrich chemicals (St. Louis, Missouri, USA). 5,5-dithiobis[2-nitrobenzoic acid] (DTNB) was purchased from Nacalai Tesque (Kyoto, Kyoto Prefecture, Japan). Donepezil and tacrine hydrochloride were purchased from Cayman Chemical (Ann Arbor, Michigan, USA), whereas galantamine hydrobromide was purchased from Tocris Biosciences (Bristol, UK). Assays were performed in Greiner Bio-One (Kremsmünster, Austria) 96-well plate.

Ellman's method was used to determine the cholinesterase inhibition activity of test compounds. All stock solutions were prepared at 10 mM in 100% DMSO and the final concentration of DMSO was maintained at 1%. Briefly, the AChE inhibition assay started with the addition of 140 µL of 0.1 M phosphate buffer saline (pH 7.8) in the well in 96-well plate, followed by the addition of 20 µL test compounds (in 10% DMSO), then the 0.1 unit/mL AChE (dissolved and diluted in PBS). A 15 min pre-incubation under room temperature was done before the addition of 10 mM DTNB (dissolved in PBS) and 14 mM acetylthiocholine iodide. Absorbance was measured using Tecan Infinite M200 microplate

reader (Tecan, Männedorf, Switzerland). Absorbance measurement at 412 nm was done after 45 min incubation under room temperature. For BChE inhibition assay, AChE and acetylthiocholine iodide were replaced by BChE and S-butyrylthiocholine iodide, respectively. Absorbance of each derivative was normalized by subtracting their respective blanks. The 50% inhibitory concentration (IC_{50}) determination of derivatives involved a set of six concentrations, conducted in quadruplicate and two biological replications. The value was expressed as mean ± standard deviation.

Mode of binding

Lineweaver–Burk plots were carried out to determine the enzyme kinetics and the mode of enzyme inhibition by compound **3 h** against the cholinesterase enzymes. Lineweaver–Burk plots were plotted at varying inhibitor concentrations (0 µM, IC_{50}, $2 \times IC_{50}$) and varying substrate concentrations. The type of inhibition and kinetic parameters such as maximum velocity (V_{max}) and Michaelis–Menten constant (K_m) were determined using the Michaelis–Menten equation from the Lineweaver–Burk plot. The inhibitor constant (K_i) was determined from a secondary (Dixon) plot obtained from the Lineweaver–Burk plot. Each test was conducted in triplicates.

Antiproliferative assay

The liver hepatocellular carcinoma cell line (HepG2) was obtained from ATCC (Old Town Manassas, Virginia, USA). Dulbecco's Modified Eagle Media (DMEM) high glucose without pyruvate supplement was purchased from Gibco, Thermo Fisher Scientific (Waltham, Massachusetts, USA). The media was supplemented with 10% foetal bovine serum (FBS) and 1% penicillin–streptomycin from Gibco, Thermo Fisher Scientific (Waltham, Massachusetts, USA). The 3-(4,5-Dimethyl-2-thiazolyl)-2,5-diphenyl-2H-tetrazolium bromide (MTT) reagent was purchased from Merck (Kenilworth, New Jersey, USA). Dimethyl sulfoxide (DMSO) was obtained from Nacalai Tesque (Kyoto, Kyoto Prefecture, Japan). Assays were performed in Greiner Bio-One (Kremsmünster, Austria) 96-well plate.

Briefly, HepG2 cells were cultured in a 96-well plate with 5000 cells/well density. After adherence, the cells were treated with 10 µM of compounds. The cell viability after 24 h of incubation (37 °C, 5% CO_2) in treatment well was determined using MTT reagent. A concentration of 0.05 mg/mL MTT reagent was used in each treatment well and was proceeded to 4 h incubation before the measurement. Cell culture medium with MTT reagent was aspirated from each treatment well and DMSO was added to dissolve the formazan crystals. Absorbance was measured using Tecan Infinite M200 microplate reader (Tecan, Männedorf, Switzerland) at 590 nm. The 50% growth inhibition (GI_{50}) determination of derivatives involved a set of five concentrations, conducted in triplicate and two biological replications. The value was expressed as mean ± standard deviation.

Molecular docking

Docking simulations were performed using the Genetic Algorithm(GA) method provided in the Autodock 4.2 [14] software. First, BChE (PDB ID: 1P0I) [15] crystal structure was retrieved from the Protein Data Bank. Autodock 4.2 software was used for protein and ligand preparations. Control docking studies were performed for validation of methods. Polar hydrogens were added and water molecules were deleted. Gasteiger charge was applied while the ligand (butanoic acid) was removed. Other parameters were applied as default. In this regard, 2,500,000 maximum number of evaluations, 10 GA runs and 27,000 maximum number of generations were employed. The best pose of the largest cluster was chosen for each ligand. After the method was validated, ligands were docked into the active sites of the BChE enzymes. Ligand interactions were examined in Discovery Studio Visualizer software [16].

In silico *ADME*

ADME and molecular properties were calculated via Discovery Studio 3.5. The investigated properties are molecular weight, AlogP and aqueous solubility. The first two rules are according to Lipinski's rule of five [17] and aqueous solubility value was the value that Cheng and Merz classified as soluble [18].

Results and discussion

Chemistry

The reaction scheme was adapted from Akı-Şener et al. [13]. Benzimidazoles with carboxamide and carbohydrazide were successfully synthesized with facile conditions and easily recrystallized using ethanol. In the first step, various substituted benzaldehydes were changed to their respective sodium salt adducts for ease of purification before subsequent reaction with 3,4-diaminobenzoic acid to yield the benzimidazole scaffold. This reaction scheme yielded 19–50% of 22 final products, followed by characterization by nuclear magnetic resonance (NMR) and mass spectrometry. Figures 1 and 2 show the reaction schemes for compounds synthesized in this study.

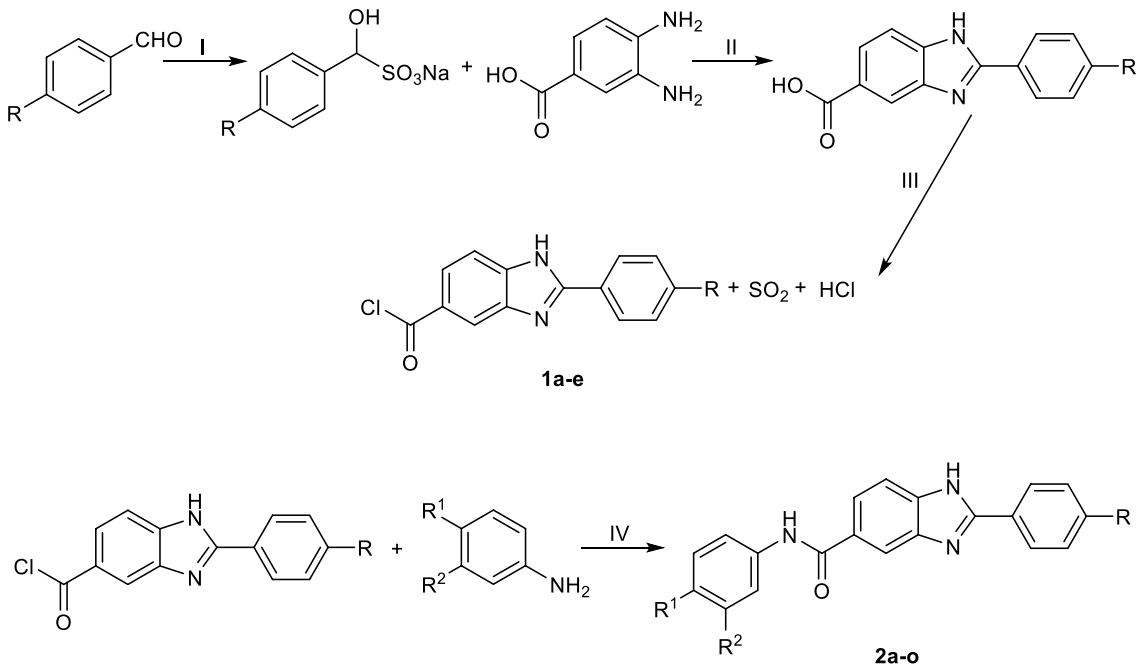

1a-1e; R: -OH, -OCH_3, CH_3, Br,

2a-2r; R^1: -OH, -OCH_3, Cl, Br, **R^2:** -H, -CF_3, -OCH_3, -NO_2

Fig. 1 Synthetic pathway of 2-(4-substituedphenyl)-N-(3/4-substituedphenyl)-1H-benzimidazole-5-carboxamide derivatives. Reagents and conditions: (I) $Na_2S_2O_5$; (II) DMF, 100–120 °C, 1.5–2.5 h; (III) $SOCl_2$, 80 °C, 4 h; (IV) $NaHCO_3/H_2O$/Diethyl ether, 0–5 °C, overnight. **1a-e; R:** –OH, –OCH_3, CH_3, Br, **2a-2r; R^1:** –OH, –OCH_3, Cl, Br, **R^2:** –H, –CF_3, –OCH_3, –NO_2

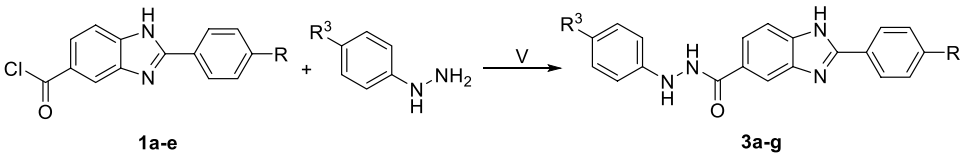

3a-3g; R^3: -NO_2, -Br, -Cl

Fig. 2 Synthetic pathway of 2-(4-substituedphenyl)-N-(4-substituedphenyl)-1H-benzimidazole-5-carbohydrazide derivatives. Reagents and conditions: (V) $NaHCO_3/H_2O$/Diethyl ether, 0–5 °C, overnight. **3a-g; R^3:** –NO_2, –Br, –Cl

Cholinesterase inhibitory activity

All synthesized compounds were analysed for cholinesterase inhibitory activity using modified Ellman's method. Donepezil was used as the reference standard for AChE while galantamine was used as the reference standard for BChE. Previously, benzimidazole derivatives have been shown to act as cholinesterase inhibitors [17]. The current study explores the potential of various other substitutions to the benzimidazole core structure to generate potent cholinesterase inhibitors. All compounds synthesized were screened at 10 µM and the results are tabulated in Table 1. The half maximal inhibitory concentration (IC_{50}) values were then determined for selected compounds, which showed more than 80% inhibition during the initial screening process (Table 2). In general, the screened compounds demonstrated better BChE inhibitory activity than AChE inhibitory activity, with the AChE inhibitory activity mostly below 50% (at 10 µM) except for **2 g**. Compound **2 g** showed the best AChE inhibitory activity but only at moderately potent level (67.8% at 10 µM). The only dibromo compound presented here, **3 g** showed moderate BChE inhibitory activity (70.8%) when screened at 10 µM. All three compounds which were selected (**2c**, **2j** and **3f**) for IC_{50} determination were selective BChE inhibitors, with at least 30-fold selectivity against BChE than AChE. Among all, compound **2j** and **3f** are the best BChE inhibitors with comparable potency (IC_{50} = 1.13 µM and 1.46 µM, respectively) while compound **2c** was found to be slightly less potent (IC_{50} = 2.94 µM). They were more potent than galantamine and donepezil against BChE, thereby

Table 1 Cholinesterase inhibitory activity of compounds

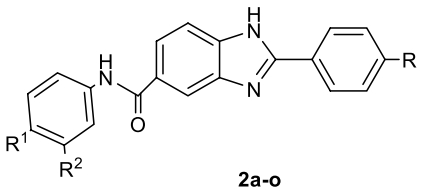

2a-o

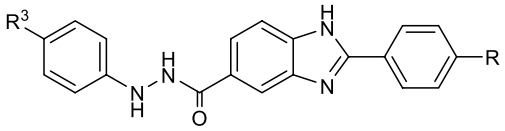

3a-g

Compound	R	R^1	R^2	R^3	AChE inhibition at 10 μM (%)	BChE inhibition at 10 μM (%)
2a	–OH	–Cl	–H	–	NI[a]	25.4 ± 1.8
2b	–OH	$–OCH_3$	–H	–	22.7 ± 4.5	29.2 ± 2.4
2c	–OH	–H	$–CF_3$	–	12.4 ± 2.2	85.0 ± 11.3
2d	$–OCH_3$	$–OCH_3$	–H	–	19.0 ± 2.7	NI
2e	$–OCH_3$	–Cl	–H	–	43.2 ± 6.4	47.5 ± 5.9
2f	$–OCH_3$	–OH	–H	–	NI	26.1 ± 3.1
2 g	$–OCH_3$	–Br	–H	–	67.8	15.7
2 h	$–OCH_3$	–H	$–OCH_3$	–	17.6 ± 3.8	32.3 ± 3.0
2i	$–CH_3$	–Cl	–H	–	14.5 ± 4.3	28.7 ± 5.5
2j	$–CH_3$	–OH	–H	–	11.0 ± 7.4	84.5 ± 5.5
2 k	$–CH_3$	$–OCH_3$	–H	–	NI	18.4 ± 3.4
2 l	$–CH_3$	–H	$–OCH_3$	–	37.8 ± 2.3	41.4 ± 9.3
2 m	–Br	$–OCH_3$	–H	–	43.3	46.4
2n	–Br	–H	$–NO_2$	–	42.5 ± 5.7	52.6 ± 5.3
2o	–Br	–Cl	–H	–	47.0	35.2
3a	–OH	–	–	$–NO_2$	11.9 ± 3.8	33.3 ± 4.0
3b	$–OCH_3$	–	–	$–NO_2$	NI	40.0%
3c	$–OCH_3$	–	–	–Br	NI	44.0 ± 5.1
3d	$–OCH_3$	–	–	–Cl	12.1%	N.I
3e	$–CH_3$	–	–	–Cl	NI	23.7%
3f	$–CH_3$	–	–	–Br	49.6 ± 1.2	93.8 ± 2.0
3 g	–Br	–	–	–Br	18.0 ± 3.5	70.8 ± 8.6
Donepezil			84.3 ± 8.7 at 1 μM	6.93 ± 1.5 at 1 μM		
Galantamine			70.8 ± 6.35 at 10 μM	39.2 ± 2.9 at 10 μM		

[a]NI: No inhibition

The characters are bolded in the table as they are referring to the compound codes

Table 2 IC_{50} determination of selected compounds

Compound	IC_{50} AChE (μM)	IC_{50} BChE (μM)	Selectivity Index (IC_{50} BChE/IC_{50} AChE)
2c	> 100	2.94 ± 1.56	> 34
2j	> 100	1.13 ± 0.15	> 88
3f	> 100	1.46 ± 0.39	> 68
Donepezil	0.18 ± 0.08	–	–
Galantamine	–	4.54 ± 1.26	–

The characters are bolded in the table as they are referring to the compound codes

demonstrating their potential to be used as selective BChE inhibitors. Overall, based solely on the anticholinesterase activity, it was clear that compounds **2j** and **3f** showed the best potential. Although the compounds are substituted at various positions with electron donating, electron withdrawing and halogen groups, there was no clear trend observed in regard to their structure–activity relationship. This implies that the activity shown by the compounds is likely (at least in part) due to the steric factor rather than purely electronic factor. This is further explored using molecular docking studies.

Both **2j** and **3f** contained a methyl substitution at the R position. As shown in Table 1, there is a huge difference between the potency of these 2 compounds with their closest analogues. In comparison with **2 k**, compound **2j** has a –OH

group while **2 k** has a $–OCH_3$ group at the R^1 position. It was noted that for **2j,** the hydrogen from –OH (at R^1) is able to form a strong H bond with Gly117 (''Molecular docking'' section) which may be the reason for its strong observed activity. In comparison, **2 k** which with its $–OCH_3$ group is unable to have that interaction. Meanwhile, compound **3f** with a Br at the R^3 position fits well into the active cavity of BChE and is able to have interactions with pi-alkyl bonding with Ala328 and Trp430. Its close analogue, **3e** meanwhile lost its potency against BChE with a Cl substitution at R^3 which could be due to the smaller size of Cl atom.

Several studies have determined a correlation between the increased activity of BChE and the onset of AD. Potential therapeutics which target BChE are actively being studied. However, currently BChE inhibitors are yet to be marketed as potential therapeutics for AD [11]. In the past, BChE was thought to play a supporting role in the hydrolysis of acetylcholine. However, more recent studies examining postmortem brain samples of AD patients have identified its influence in the maturation of Aβ plaques and also its increased activity in those diagnosed with severe AD [12, 19]. An increase in activity of BChE was also observed as ageing progressed compared to AChE, thereby making the enzyme an important therapeutic target for AD [20]. Furthermore, absence of BChE activity does not lead to obvious physiological disturbance that is known to limit the use of AChE inhibitors [21].

Kinetics and mode of BChE inhibition

BChE inhibition kinetics were determined for **3f** and results are summarized as Lineweaver–Burk plot (Fig. 3) and its secondary plot and kinetic data (Supplementary Information). The results suggest that **3f** is a linear mixed-mode inhibitor of BChE, where it can bind to the enzyme's active or allosteric sites. Binding to the active site of the enzyme prevents the insertion and break down of substrate. In contrast, a mixed-inhibitor may also bind to allosteric sites causing changes in the shape of the enzyme and reduces its activity. The estimated K_i value was 0.84, which implied strong binding between the **3f** and the enzyme.

Molecular docking

Interested ligands (**2c**, **2j** and **3f**) were docked into the active site of the BChE (PDB: 1P0I) enzyme. The ligands were drawn in Discovery Studio Visualizer [16] and converted into pdbqt files with OpenBabel software. The results are presented in Table 3 and depicted in Figs. 4, 5, 6, 7. Control docking studies were performed with BUA to validate the molecular docking. BUA exhibited good interactions with the BChE enzyme. It interacted with the enzyme with four conventional hydrogen bonds (Gly116, Gly117, Ala199, His438) and a pi-sigma interaction with Trp231. Crystal structure of BChE with some ligands complexed in it also had similar non-covalent interactions at most of the residues detected in the molecular docking as mentioned in the alternative binding suggested previously [15]. Hence, the molecular docking results in this study fit with the experimental binding analysis outcomes reported. Together with the binding similarity between the standard binding ligand (BUA) and the active compounds in the computational analysis, this result validated the docking process. In addition to this, RMSD was calculated with the superimposition of BUA in the crystal structure and the docked one to

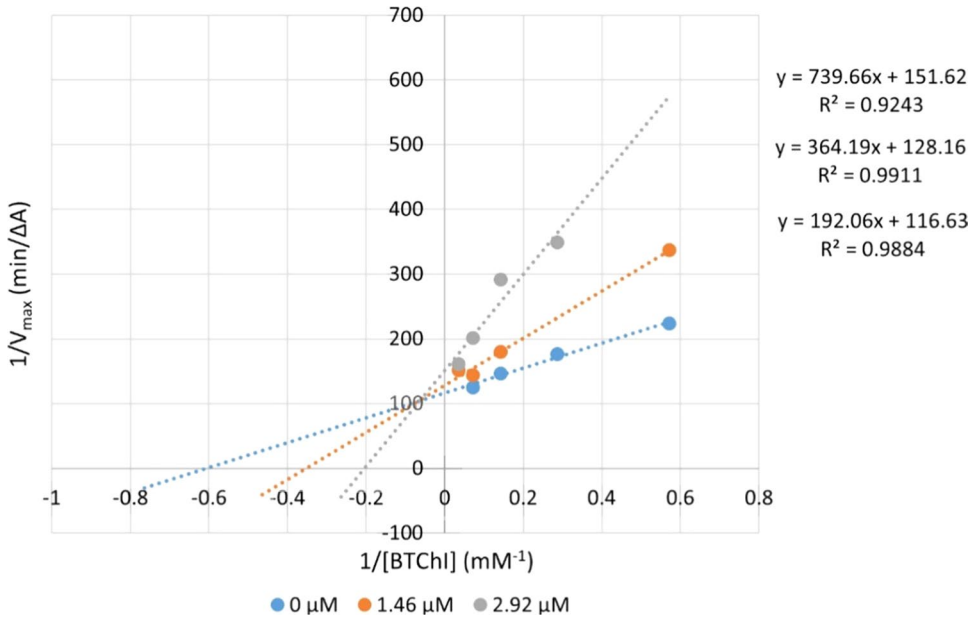

Fig. 3 Lineweaver–Burk plot of BChE inhibition by compound 3f

Table 3 Docking results with human BChE enzyme

Compound	Binding energy (kcal/mol)	Hydrogen bond	Other interactions
BUA	−4.64	Gly116, Gly117, Ala199, His438	Trp231[a]
2c	−9.0	His438	Ile69[b], Asp70[c], Trp82[b], Gly116 (2)[d], Ala328[e], Tyr332(2)[b]
2j	−9.4	Ser198, Ser287, Tyr332, His438	Trp82[b], Gly116(2)[c], Gly117[f]
3f	−10.5	Trp82, Trp430, His438, Tyr440	Ile69[b], Asp70[c], Trp82[b], Gly115[g], Ala328[e], Tyr332(2)[b], His438[c]

[a]pi-sigma; [b]pi-pi; [c]pi-ion; [d]carbon hydrogen bond; [e]pi/alkyl-alkyl; [f]van der Waals; [g]halogen interactions
The characters are bolded in the table as they are referring to the compound codes

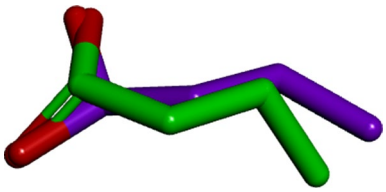

Fig. 4 Structural superimposition of the docked BUA (purple) and from the crystal structure (green); RMSD = 0.65 Å (for heavy atoms)

assess their similarity. The outcome was an acceptable value (RMSD = 0.65 Å) (Fig. 4).

Compound **3f** was found to have better affinity towards BChE although all the three compounds were found to bind to the active site of BChE. This difference in affinity could be due to the conformation of the compounds in the active site. Compound **3f** was demonstrated to form strong hydrogen bond with His438, which is catalytic residue for the enzyme. Compounds **2c** and **2j** also had hydrogen bond with His438. Compound **3f** formed hydrogen bond with Trp82 at the choline binding pocket and pi-alkyl interaction with Ala328 at the oxyanion hole, which are also important amino acids responsible for activity of the enzyme [22]. Similarly, compound **2c** had similar interactions with these residues and **2j** also had similar interaction with Trp82. Although compounds **2j** and **3f** had four hydrogen bonds **3f** interacted slightly stronger than **2j**. Furthermore, the similarity between binding residues of **2j** and the standard molecule in the crystal structure of BChE was higher than **3f**. In general, the level of the interactions of the active ligands detected in the computational analysis was compatible with the experimental inhibition activity results (Tables 2, 3).

Histidine plays an important role as catalytic residue in enzymatic active sites [23]. Since its side chain p*K*a (around 6) is close to the physiological pH, small changes in the

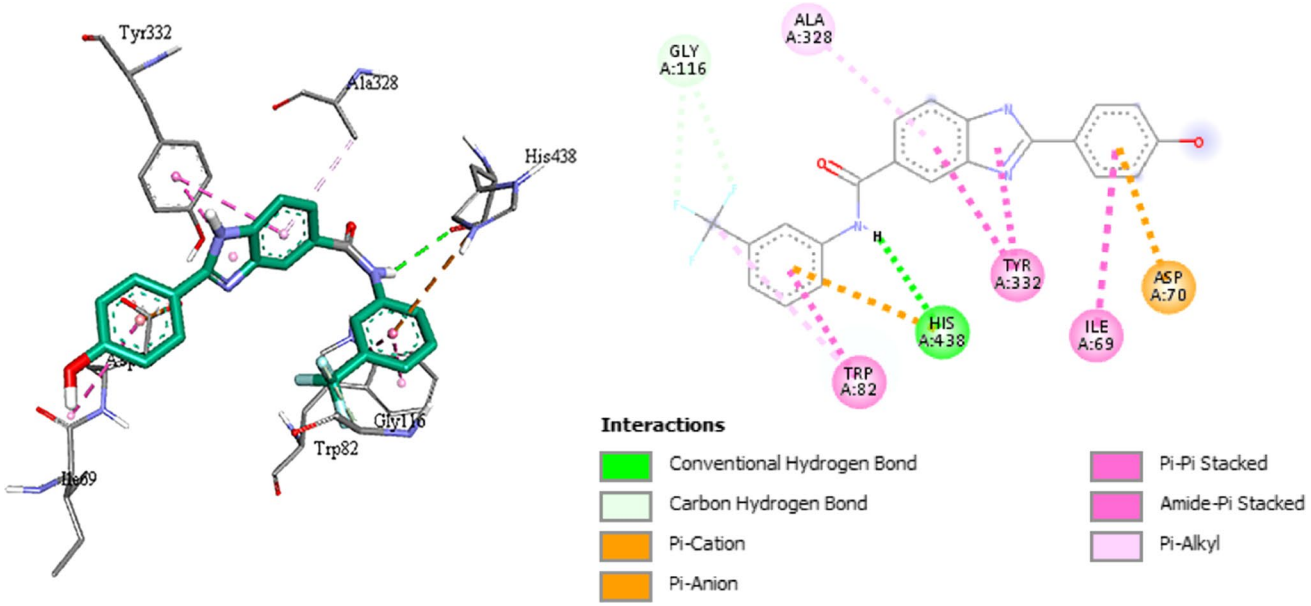

Fig. 5 Compound **2c** in the binding site of BChE enzyme. 2D ligand interaction diagram of **2c**-BChE enzyme is as shown

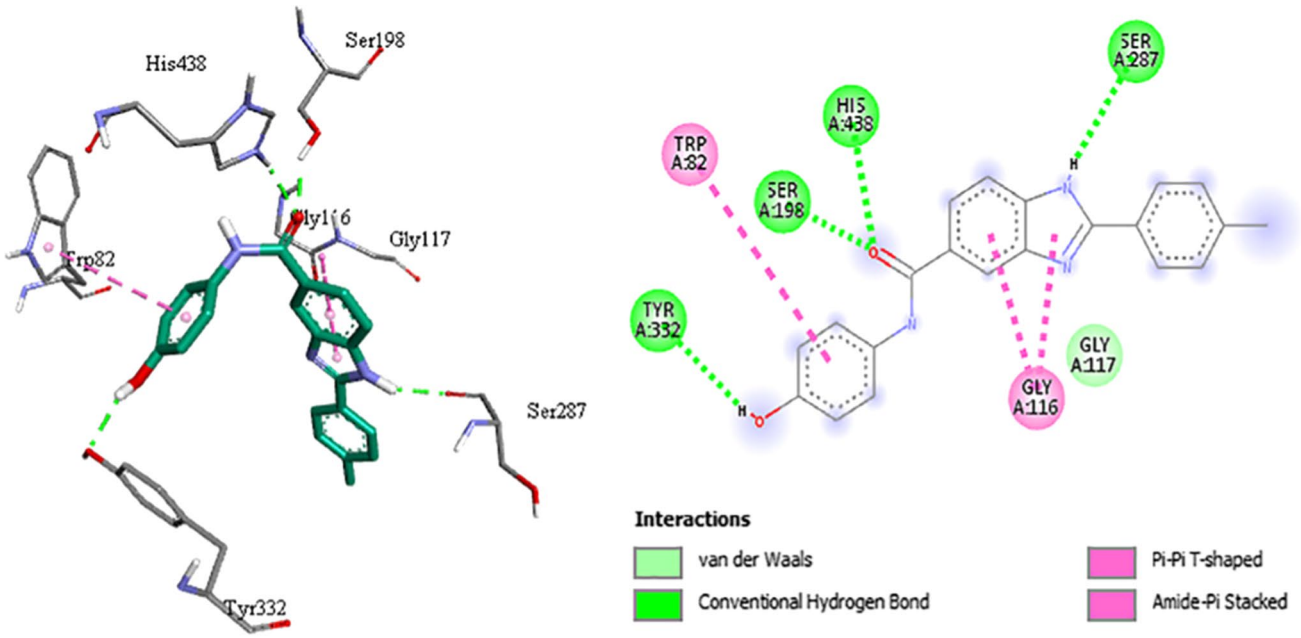

Fig. 6 Compound **2j** in the binding site of BChE enzyme. 2D ligand interaction diagram of **2j**-BChE enzyme is as shown

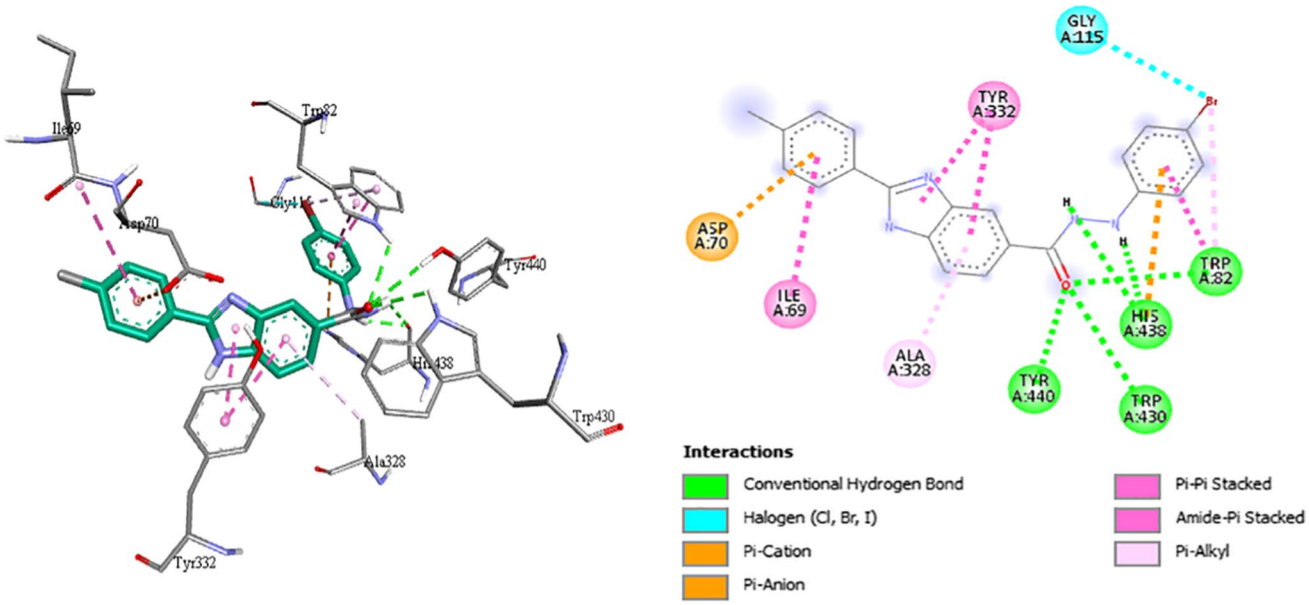

Fig. 7 Compound **3f** in the binding site of BChE enzyme. 2D ligand interaction diagram of **3f**-BChE enzyme is as shown

environmental pH can readily change the histidine charged state [24]. At low pH, both nitrogen of imidazole are protonated to give positive charge amino acid (HIP). At high pH, the histidine is neutral with protonated δ-nitrogen (HID) or ε-nitrogen (HIE) [25]. In the protein structure used for molecular docking, His438 is among the residues in the active site. Thus, theoretical calculation of the pH of the amino acid environment was undertaken with PROPKA [26]. The environment of His438 was predicted to be slightly basic with the hit ligands in it. Hence, His438 is expected to be neutral. Neutral histidine can serve as a general base [24]. In this computational study, at least an interaction of histidine with the hit ligands was detected. In the interaction of His438 with **2c** and **3f**, the histidine was found to act as hydrogen bond acceptor. In the rest of its interactions with the hit ligands, the single nitrogen protonated histidine (HID,

Table 4 ADME prediction of hit and reference compounds towards the BBB

Compounds	AquSolubility	Solubility Level	ADMET_BBB	BBB Level	ALogP	PSA_2D
2c	−6.474	1	0.094	1	4.755	77.242
2j	−5.280	2	−0.047	2	4.299	77.242
3f	−6.547	1	0.392	1	5.312	69.237
Donepezil	−5.504	2	0.649	1	4.569	38.513
Galantamine	−3.001	3	−0.373	2	1.442	42.028

The characters are bolded in the table as they are referring to the compound codes

HIE) took part in the pi-cation interactions. The interaction profile of His438 was as anticipated that resulted from its diverse protonation states.

ADME prediction

Synthesized compounds agreed with the Lipinski's rule of five, which is developed for predicting the drug-likeness property of a small molecule. Polar surface area was also calculated and blood–brain penetration model was prepared via Discovery Studio 3.5. PSA less than 70 $Å^2$ is considered suitable for a compound to pass through the blood–brain barrier (BBB) [27].

Accelrys recently developed robust model for the prediction of BBB penetration. This model predicts BBB penetration after oral administration. They were derived from over 800 compounds that are known to enter the central nervous system (CNS) after oral administration [28]. This model was used for calculation of BBB level via Discovery Studio 3.5 software [16]. BBB level 1 represents high penetration while level 2 is medium.

The target BChE resides deep in the brain, protected by the highly selective semipermeable border made up of endothelial cells [29]. Drugs targeting the central nervous system must be designed such that they can pass through the barrier and deliver the therapeutic effects. The results predicted that the hit compounds (**2c**, **2j**, **3f**) and references (galantamine, donepezil) are aqueous soluble and have relatively good BBB permeability. These results augur well for compounds which targets the CNS, especially the brain. In addition to this, PSA_2D outcomes for all the ligands were found to be below 100 (Table 4). This implies that the ligands are anticipated to have good membrane permeability. Similarly, AlogP98 outcomes for all the ligands, except for compound **3f**, were found to be below five (Table 4). This indicates that the ligands have suitable lipophilic property [30]. The results are presented in Table 4.

Antiproliferative assay

One of the most common reasons for the withdrawal of approved drugs from the market is drug-induced hepatotoxicity [31]. In fact, this was one of the main issues that have dogged tacrine which have led to its withdrawal as an AD drug in 2013. As the best compounds, **2j** and **3f,** have comparable BChE inhibitory activities, both compounds are further tested for their cytotoxicity against liver hepatoma HepG2 cells. MTT assay was used to measure cell growth and DMSO (5%) was used as positive control. Both compounds demonstrated different cytotoxicity profiles when tested up until 50 µM final concentration after 24 h incubation. Compound **3f** was demonstrated to have a better safety profile against HepG2 cells, with $GI_{50} > 50$ µM. However, compound **2j** was found to be cytotoxic with $GI_{50} = 5.19$ µM. The GI_{50} of compound **3f** is calculated to be > 30-fold greater than the concentration required to achieve 50% in vitro inhibition of BChE. In comparison to compound **2j**, compound **3f** is more promising for further development.

Conclusion

Most of the compounds are broadly better in inhibiting BChE than AChE. Of all the compounds that were screened, compounds **2c, 2j, 3f, 3 g** were identified as the most potent inhibitors for BChE. Afterwards, compounds **2c**, **2j** and **3f** were further screened to determine the IC_{50} values on both AChE and BChE and compound **2j** and **3f** were found most active on BChE. The compounds were also selective towards BChE. Unlike **2j,** antiproliferative studies carried out indicated that compound **3f** showed good preliminary safety profile. Furthermore, molecular docking studies carried out indicated that the compound was bound within the enzyme active site with important interactions with several amino acids. Compound **3f** was also predicted to have high penetration across the BBB. Taken together, compound **3f** showed good potential to be used as a selective BChE inhibitor for AD treatment.

Supplementary Information The online version contains supplementary material available at https://doi.org/10.1007/s11030-022-10476-8.

Acknowledgements The authors would like to thank School of Science, Monash University Malaysia, for supporting this work. This

work was funded through Monash University Malaysia Early Career Researcher Seed Fund (ECRG-2019-10-SCI).

Authors contributions Keng Yoon Yeong and Esin-Aki Yalcin conceptualized the project. Material preparation and data collection were performed by Ozum Ozturk, Fathima Manaal Farouk, Luyi Ooi, Christine Shing Wei Law and Muhammed Tilahun Muhammed. Data analyses were performed by all authors. All authors read and approved the manuscript.

Availability of data and materials Compound characterization data including NMR and mass spectra for all compounds, detailed cholinesterase inhibition and compound cytotoxic information are available in Supplementary Data.

Declarations

Conflict of interest There are no conflicts to declare.

Code availability Not applicable.

Ethics approval Not applicable.

References

1. Farouk FM, Ooi L, Law CSW, Yeong KY (2020) Dual-target-directed ligand displaying selective butyrylcholinesterase inhibitory and neurite promoting activities as a potential therapeutic for Alzheimer's disease. ChemistrySelect 5:11229–11236. https://doi.org/10.1002/slct.202001202
2. Hampel H, Mesulam MM, Cuello AC, Farlow MR, Giacobini E, Grossberg GT, Khachaturian AS, Vergallo A, Cavedo E, Snyder PJ, Khachaturian ZS (2018) The cholinergic system in the pathophysiology and treatment of Alzheimer's disease. Brain 141(7):1917–1933. https://doi.org/10.1093/brain/awy132
3. Cummings J, Lee G, Ritter A, Sabbagh M, Zhong K (2019) Alzheimer's disease drug development pipeline: 2019. Alzheimer's Dement Transl Res Clin Interv 5:272–293. https://doi.org/10.1016/j.trci.2019.05.008
4. Godoy JA, Rios JA, Zolezzi JM, Braidy N, Inestrosa NC (2014) Signaling pathway cross talk in Alzheimer's disease. Cell Commun Signal 12(1):1–12. https://doi.org/10.1186/1478-811X-12-23
5. Ramos-Rodriguez JJ, Pacheco-Herrero M, Thyssen D, Murillo-Carretero MI, Berrocoso E, Spires-Jones TL, Bacskai BJ, Garcia-Alloza M (2014) Rapid β-amyloid deposition and cognitive impairment after cholinergic denervation in APP/PS1 mice. J Neuropathol Exp Neurol 72(4):272–285. https://doi.org/10.1097/NEN.0b013e318288a8dd
6. Sharma K (2019) Cholinesterase inhibitors as Alzheimer's therapeutics (review). Mol Med Rep 20(2):1479–1487. https://doi.org/10.3892/mmr.2019.10374
7. Xu M, Peng Y, Zhu L, Wang S, Ji J, Rakesh KP (2019) Triazole derivatives as inhibitors of Alzheimer's disease: current developments and structure-activity relationships. Eur J Med Chem 180:656–672. https://doi.org/10.1016/j.ejmech.2019.07.059
8. Ha ZY, Ong HC, Oo CW, Yeong KY (2020) Synthesis, molecular docking, and biological evaluation of benzimidazole derivatives as selective butyrylcholinesterase inhibitors. Curr Alzheimer Res 17:1177–1185. https://doi.org/10.2174/1567205018666210218151228
9. Cevik UA, Saglik BN, Levent S, Osmaniye D, Cavuşoglu BK, Ozkay Y, Kaplancikli ZA (2019) Synthesis and AChE-inhibitory activity of new benzimidazole derivatives. Molecules 24(5):861. https://doi.org/10.3390/molecules24050861
10. Yeong KY, Ali MA, Ang CW, Tan SC, Khaw KY, Murugaiyah V, Osman H, Masand VH (2013) Synthesis, characterization, and molecular docking analysis of novel benzimidazole derivatives as cholinesterase inhibitors. Bioorg Chem 49:33–39. https://doi.org/10.1016/j.bioorg.2013.06.008
11. Ha ZY, Mathew S, Yeong KY (2019) Butyrylcholinesterase: a multifaceted pharmacological target and tool. Curr Protein Pept Sci 21(1):99–109. https://doi.org/10.2174/1389203720666191107094949
12. Greig NH, Utsuki T, Ingram DK, Wang Y, Pepeu G, Scali C, Yu QS, Mamczarz J, Holloway HW, Giordano T, Chen D, Furukawa K, Sambamurti K, Brossi A, Lahiri DK (2005) Selective butyrylcholinesterase inhibition elevates brain acetylcholine, augments learning and lowers Alzheimer beta-amyloid peptide in rodent. Proc Natl Acad Sci USA 102(47):17213–17218. https://doi.org/10.1073/pnas.0508575102
13. Akı-Şener E, Bingöl KK, Temiz-Arpaci Ö, Yalçn I, Altanlar N (2002) Synthesis and microbiological activity of some N-(2-hydroxy-4-substitutedphenyl)benzamides, phenylacetamides and furamides as the possible metabolites of antimicrobial active benzoxazoles. Farmaco 57(6):451–456. https://doi.org/10.1016/S0014-827X(02)01226-0
14. Morris GM, Huey R, Lindstrom W, Sanner MF, Belew RK, Goodsell DS, Olson AJ (2010) AutoDock4 and AutoDockTools4: automated docking with selective receptor flexibility. J Comput Chem 30(16):2785–2791. https://doi.org/10.1002/jcc.21256
15. Nicolet Y, Lockridge O, Masson P, Fontecilla-Camps JC, Nachon F (2003) Crystal structure of human butyrylcholinesterase and of its complexes with substrate and products. J Biol Chem 278(42):41141–41147. https://doi.org/10.1074/jbc.M210241200
16. Discovery Studio Predictive Science Application | Dassault Systèmes BIOVIA
17. Lipinski CA, Lombardo F, Dominy BW, Feeney PJ (2012) Experimental and computational approaches to estimate solubility and permeability in drug discovery and development settings. Adv Drug Deliv Rev 46(1–3):3–26. https://doi.org/10.1016/S0169-409X(00)00129-0
18. Cheng A, Merz KM (2003) Prediction of aqueous solubility of a diverse set of compounds using quantitative structure-property relationships. J Med Chem 46(17):3572–3580. https://doi.org/10.1021/jm020266b
19. Tasker A, Perry EK, Ballard CG (2005) Butyrylcholinesterase: impact on symptoms and progression of cognitive impairment. Expert Rev Neurother 5(1):101–106. https://doi.org/10.1586/14737175.5.1.101
20. Greig NH, Utsuki T, Yu Q, Zhu X, Holloway HW, Perry T, Lee B, Ingram DK, Lahiri DKA (2001) A new therapeutic target in Alzheimer's disease treatment: attention to butyrylcholinesterase. Curr Med Res Opin 17(3):159–165. https://doi.org/10.1185/03007990391170 57
21. Li B, Duysen EG, Lockridge O (2008) The butyrylcholinesterase knockout mouse is obese on a high-fat diet. Chem Biol Interact 175(1–3):88–91. https://doi.org/10.1016/j.cbi.2008.03.009
22. Vyas S, Beck JM, Xia S, Zhang J (2010) Butyrylcholinesterase and G116H, G116S, G117H, G117N, E197Q and G117H/E197Q mutants: a molecular dynamics study. Chem Biol Interact 187(1–3):241–245. https://doi.org/10.1016/j.cbi.2010.04.004
23. Dokainish HM, Kitao A (2016) Computational assignment of the histidine protonation state in (6–4) photolyase enzyme and its effect on the protonation step. ACS Catal 6:55000–55507. https://doi.org/10.1021/acscatal.6b01094

24. Li S, Hong M (2011) Protonation, tautomerization, and rotameric structure of histidine: a comprehensive study by magic-angle-spinning solid-state NMR. J Am Chem Soc 133:1534–1544. https://doi.org/10.1021/ja108943n
25. Kim MO, Nichols SE, Wang Y, McCammon JA (2013) Effects of histidine protonation and rotameric states on virtual screening of M. tuberculosis RmlC. J Comput Aided Mol Des 27:235–246. https://doi.org/10.1007/s10822-013-9643-9
26. Olsson MHM, Søndergaard CR, Rostkowski M, Jensen JH (2011) PROPKA3: Consistent treatment of internal and surface residues in empirical p K a predictions. J Chem Theory Comput 7:525–537. https://doi.org/10.1021/ct100578z
27. Pajouhesh H, Lenz GR (2005) Medicinal chemical properties of successful central nervous system drugs. NeuroRx 2(4):541–553. https://doi.org/10.1602/neurorx.2.4.541
28. Egan WJ, Lauri G (2002) Prediction of intestinal permeability. Adv Drug Deliv Rev 54(3):273–289. https://doi.org/10.1016/S0169-409X(02)00004-2
29. Alavijeh M, Chishty M, Qaiser M, Palmer A (2005) Drug metabolism and pharmacokinetics, the blood-brain barrier, and central nervous system drug discovery. NeuroRx 2(4):554–571. https://doi.org/10.1602/neurorx.2.4.554
30. Muhammed MT, Kuyucuklu G, Kaynak-Onurdag F, Aki-Yalcin E (2022) Synthesis, antimicrobial activity, and molecular modeling studies of some benzoxazole derivatives. Lett Drug Des Discov 19:1–12. https://doi.org/10.2174/1570180819666220408133643
31. Foster AJ, Chouhan B, Regan SL, Rollison H, Amberntsson S, Andersson LC, Srivastava A, Darnell M, Cairns J, Lazic SE, Jang KJ, Petropolis DB, Kodella K, Rubins JE, Williams D, Hamilton GA, Ewart L, Morgan P (2019) Integrated in vitro models for hepatic safety and metabolism: evaluation of a human liver-chip and liver spheroid. Arch Toxicol 93(4):1021–1037. https://doi.org/10.1007/s00204-019-02427-4

Authors and Affiliations

Ozum Ozturk[2] · Fathima Manaal Farouk[1] · Luyi Ooi[1] · Christine Shing Wei Law[1] · Muhammed Tilahun Muhammed[3] · Esin Aki-Yalcin[2] · Keng Yoon Yeong[1]

✉ Esin Aki-Yalcin
Esin.Aki@ankara.edu.tr

✉ Keng Yoon Yeong
yeong.kengyoon@monash.edu

[1] School of Science, Monash University Malaysia Campus, Jalan Lagoon Selatan, 47500 Bandar Sunway, Selangor, Malaysia

[2] Faculty of Pharmacy, Pharmaceutical Chemistry Department, Ankara University, 06100 Tandogan, Ankara, Turkey

[3] Department of Pharmaceutical Chemistry, Faculty of Pharmacy, Suleyman Demirel University, 32200 Isparta, Turkey